

See discussions, stats, and author profiles for this publication at: <https://www.researchgate.net/publication/231698551>

Study of Intercalation and Exfoliation Processes in Polymer Nanocomposites

ARTICLE *in* MACROMOLECULES · MAY 2006

Impact Factor: 5.8 · DOI: 10.1021/ma052647f

CITATIONS

79

READS

59

1 AUTHOR:



Mosto Bousmina

Euro-Mediterranean Université of Fez

217 PUBLICATIONS **5,343** CITATIONS

SEE PROFILE

Study of Intercalation and Exfoliation Processes in Polymer Nanocomposites

Mosto Bousmina*

Department of Chemical Engineering, CREPEC, Canada
Research Chair on Polymer Physics and Nanomaterials,
Steacie Fellowship, Laval University, Ste-Foy,
Quebec G1C 7P4, Canada

Received December 11, 2005

Revised Manuscript Received April 24, 2006

Introduction

The incorporation of a small amount of clay particles (2–6 wt %) into a thermoplastic polymeric matrix can generate enhanced properties such as thermal and UV resistance, low permeability toward gases, and to some extent improved mechanical properties.¹

The enhancement of properties is obtained through exfoliation and dispersion/distribution of clay lamellae inside the polymeric matrix. Such exfoliation is obtained through at least three routes: (i) in-situ intercalative–exfoliative polymerization, (ii) common solvent; (iii) and melt intercalation–exfoliation. The third route is privileged due to its industrial advantages without use of solvents.

The first step of the process involves modification of clay surface through for instance cation exchange that renders the surface organophilic. Such modification expands the d spacing of the clay galleries from a distance of approximately 1 to 3–4 nm. Such initial intercalated structure is believed to be necessary to allow polymeric chains to penetrate the galleries and to exert local stresses that would exfoliate the structure when the nanocomposite is submitted to mechanical shearing. Generally, modified clays are mixed in a molten state with a given polymer that is compatible with the surfactant used for the modification of clay surface. The mixing process is usually carried out in a batch mixer or alternatively in a continuous process such as extrusion. The shear is believed to be the main flow that generates high level of exfoliation. However, Utracki¹ patented a new device based rather on elongational flow that has been shown to give high exfoliation level of clay nanoparticles within thermoplastic polymers hosts.

Irrespective of the nature of the flow, high stresses and some times high strains were pointed out as the key parameters for destroying the clay galleries and dispersing the individual clay lamellae within the polymer matrix. Such a high level of individual clay lamellae dispersion and distribution is presumed to impart the final nanocomposite with enhanced mechanical properties. Dennis et al.² carried out a series of experiments on processing of polymer nanocomposites and concluded that the main important factor for exfoliation is the time and therefore the strain rather than shear stress. However, the authors used a rather rough expression for the residence time and compared different situations with different flow conditions. In fact, in their experiments all the parameters vary at the same time (nature of flow, the dominant shear rate, shear strain, and shear stress) and not only the residence time. Therefore, it is impossible to draw rigorous conclusions from the obtained

results. Additionally, contradictory conclusions were given by Fornes et al.,³ who used organoclay nanocomposites based on clay and three different molecular weights of polyamide 6. The authors concluded that the degree of exfoliation increases with molecular weight of the polyamide matrix and therefore with the shear stress that plays a dominant role. Opposite results were reported by Woo Kim et al.⁴ on a quite similar system. In fact, the authors found that a high degree of platelets delamination is obtained with a rather low viscous polyamide matrix (low shear stress). The authors explained their results by a diffusion-controlled process that requires low viscosity of the matrix. Such a conclusion sounds convincing and involves a balance between diffusion process and mechanical shearing. Nassar et al.⁵ and also Tanoue et al.⁶ used different grades of polystyrene with different molecular weights in the presence of clay and found that low molecular weight or lower viscosity polystyrene resins exhibit higher degrees of intercalation.

The main objective of this work is to discuss the physics of both intercalation and exfoliation processes and to examine the conditions that lead to a higher level of clay exfoliation in flexible polymer matrixes. The question to be answered is whether low or high shear stresses are required for exfoliation. Our analysis will be supported by providing theoretical and experimental arguments using the state-of-the art experimental design.

Intercalation

Clay belongs to the family of phyllosilicates. The most used clay in polymer nanocomposites is montmorillonite (MMT) having the following chemical composition $(\text{Al}_{2-y}\text{Mg}_y)(\text{Si}_{4-x}\text{Al}_x)\text{O}_{10}(\text{OH})_2\text{M}_y^+$. M^+ is the cation (sodium or calcium), and y is the degree of substitution. Let us now estimate the energy of adhesion between the MMT–lamellae assuming flat plates having both a length $L = 100$ nm and a thickness $t = 1$ nm separated by a distance d . The perfect superimposed flat plates are supposed to interact via the most general potential energy:⁷

$$E = 64k_{\text{B}}Tn_0\bar{\lambda}^2 \exp(-\kappa d) + \frac{A_{\text{H}}L^2}{12\pi} \left[\frac{1}{d^2} + \frac{1}{(2t+d)^2} - \frac{2}{(t+d)^2} \right] + \frac{1}{(4\pi\epsilon_0 d^3)^2} \left[\left(m_1^2 \mathcal{P}_2 + m_2^2 \mathcal{P}_1 + \frac{m_1^2 m_2^2}{3k_{\text{B}}T} + \frac{3h\mathcal{P}_1\mathcal{P}_2\nu_1\nu_2}{2(\nu_1 + \nu_2)} \right) \right] \quad (1)$$

where m_1 and m_2 are the total permanent dipole moments of the plates 1 and 2, respectively, \mathcal{P}_i their polarizabilities, ν_i their ionization frequencies, $h = 6.626 \times 10^{-34}$ J (Planck constant), and $\epsilon_0 = 8.8 \times 10^{-12}$ C² J⁻¹ m⁻¹. A_{H} is the Hamaker constant, which is related to the surface energy, Γ , by A_{H} (in J) = $2 \times 10^{-21} \Gamma$ (mJ/m²). For clay this is equal to $A_{\text{H}} = 2 \times 10^{-20}$ J. $\bar{\lambda}$ is given by $\bar{\lambda} = \tanh(e\psi_s/4k_{\text{B}}T)$, where ψ_s is the potential at the surface, which can be calculated from the density charges bound to the surface and $e = 1.6 \times 10^{-19}$ C. The results of such calculations are summarized in Table 1.

Clearly at short distances van der Waals forces are predominant, and the energy of adhesion is larger than the energy of covalent carbon–carbon bond ($E_{\text{C-C}} \cong 84$ kcal/mol). The energy of adhesion between platelets becomes smaller than $E_{\text{C-C}}$ only when the distance of separation becomes larger than a certain

* E-mail Bousmina@gch.ulaval.ca; Tel 1-418-656-2767; Fax 1-418-656-5993.

Table 1. Energy of Interactions between Two Clay Lamellae as a Function of the Interlamellar Spacing d

d (nm)	energy of adhesion (kcal)
1	$416 > E_{c-c} \cong 84$ kcal/mol
2	$372 > E_{c-c}$
3	$212 > E_{c-c}$
4	$32 < E_{c-c}$

critical distance $d_c \approx 3.4$ nm. Therefore, to separate the clay lamellae without any modification of their surfaces in a noninteracting polymer matrix will require a high energy that will result in polymer degradation (breakup of C–C covalent bond) rather than in delamination of the lamellae. Such energy becomes smaller than E_{c-c} only in cases where the clay surface has specific interactions with the polymer matrix and/or when the distance of separation becomes larger than the critical distance d_c . The expansion of the lamellae to a distance larger than d_c is habitually obtained by cation exchange which replaces the sodium cations by quaternary ammonium salts having a critical length of aliphatic chains. Therefore, the main reason for intercalation is not only to facilitate the polymeric chains diffusion inside the clay galleries but most importantly to lower the energy of adhesion at a level which is below E_{c-c} .

Exfoliation

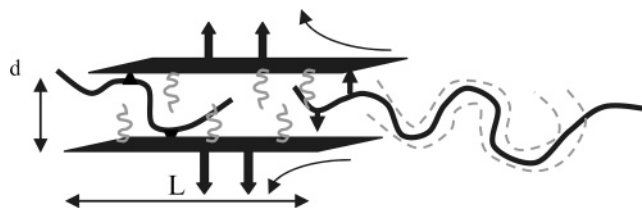
To control the state of dispersion/distribution of clay lamellae within the molten polymer during the processing step, the engineer has to identify the important processing factors such as shear rate (rpm), shear strain (time for a given rpm), and shear stress. In many cases, high mechanical energy and therefore high shear stresses are presumed to be important for destroying the compact clay structure and dispersing the individual lamellae within the polymer macromolecular network. By virtue of the generalized Newtonian relationship between shear stress, σ , and viscosity, η ($\sigma = \eta(\dot{\gamma})\dot{\gamma}$), this means that for a given shear rate, $\dot{\gamma}$, high viscosity levels would be more efficient for exfoliation. However, several experiments reported in the literature show that high viscosity levels are not always suited for exfoliation, and rather matrixes with low viscosity were found to be more efficient for exfoliation.^{4–6} There is in fact a given interval of viscosity that ensures the best level of exfoliation.

The reason is that the process of exfoliation involves not only mechanical stresses but also diffusion phenomena, with a diffusion coefficient that varies as the inverse of viscosity, $D \sim 1/\eta^a$. High viscosity of the matrix has two opposite effects. It generates high shear stresses that tend to destroy the clay galleries into individual lamellae, but at the same time it slows down the diffusion process and then makes such delamination difficult. There are two kinds of diffusion to be accounted for. The first one is the diffusion of the polymeric chains inside the confined space between the intercalated clay layers, and the second one concerns the diffusion of the lamellae within the polymeric matrix.

As pictured in Figure 1, the first diffusion process concerns the thermally activated motion of the polymeric chains inside the confined space between the lamellae. The movement of the chain is restricted by additional constraints due to (i) the confinement that exerts local stresses on the chain and (ii) eventual interactions with the intercalant agent (surfactant). The high confinement regime can be crudely characterized by a diffusion coefficient, D , given by

$$D = D_f f \quad (2)$$

where D_f is the self-diffusion coefficient of the polymer bulk

**Figure 1.** Sketch for the diffusion of polymeric chains inside the clay interlamellar galleries.

in the absence of clay. In the case of reptative chains, D_f is given by^{8–12}

$$D_f = \frac{R_{ee}^2 M_e \rho RT}{135 M^2 \eta} \quad (3)$$

R_{ee} is the end-to-end distance of the polymer with a molecular weight M . M_e is the molecular weight between entanglements, ρ is the density, η is the viscosity, R is the gas constant, and T is the temperature. f is a constraint parameter that depends on the interlamellar spacing, d , and the gyration radius, R_g . The simplest form of the function f can be derived from the scaling arguments of de Gennes^{8,13} for the stretching and self-diffusion of a chain in a thin slit of height d . In such confined channel, a chain of gyration radius $R_g \sim bN^\nu$ (N is the number of monomers of size b and $\nu = 3/5$ in a good solvent) is conceived as a string of N_b blobs containing each j monomers. The diameter of the blob is taken here equal to the height d . The number of monomers per blob is then related to d by $j \sim (d/b)^{1/\nu}$. The number of blobs is then equal to $N_b = N/j \sim (R_g/d)^{1/\nu}$. The elongation of the chain within the slit in a good solvent is given by $|\langle r \rangle| \sim dN_b^{3/4}$. This gives the following ratio:

$$\frac{|\langle r \rangle|}{R_g} \sim \frac{dN_b^{3/4}}{R_g} \sim \left(\frac{R_g}{d}\right)^{1/4} \quad (4)$$

By construction, the interactions on a scale larger than d are screened. This gives a net drag on the chain ζ that scales as^{8,13}

$$N_b \zeta_b \sim (R_g/d)^{1/\nu} d \quad (5)$$

ζ_b is the drag on the blob. Then from the scaling relation of the diffusion coefficient, D , with the gyration radius $D \sim (\eta R_g)^{-1}$, one finds the expression of the coefficient f in the strongly confined regime:

$$f \sim (R_g/d)^{-1/\nu+1} \sim (R_g/d)^{-2/3} \quad (6)$$

Equation 6 shows that the diffusion coefficient of the polymeric chain in the highly confined regime inside the interlamellar galleries is smaller than the reptation diffusion coefficient. Polymeric chains with small molecular weights diffuse more easily than chains with high molecular weight and large characteristic relaxation time. Of course, the above scaling expression (eq 6) does not include specific interactions of the diffusing chain with the surfactant used to modify the surface of clay. Such a particular situation could be accounted for by modifying the expression of the factor f by the simple form of type

$$f \sim (1 + \xi \tau S R_g^2 / \Gamma d^4)^{-\nu} \quad (7)$$

where ν is a coefficient that depends on the polymer structure, Γ is the interfacial tension, and ξ is the overall friction parameter

Table 2. Time of Diffusion of the Polymeric Chains between Two Platelets Separated by a Distance d

d (nm)	viscosity (Pa·s)	time
1	10^6	151 h
2	10^5	17 h
3	10^4	67 min
7	10^2	22 s

of the diffusing chains with both surfactant and the surface of the lamellae. Here both Γ and ζ have mean-field values.

Table 2 gives an order of magnitude of diffusion time for polymer melts with a typical values of D of 10^{-10} – 10^{-16} cm²/s. Clearly, when the d is very small and the viscosity is very high, the polymeric chains would require hundreds of hours to diffuse inside the confined space between two layers. For instance, for $d = 1$ nm and $\eta = 10^6$ Pa·s, the diffusion time is of about 150 h. Such a time drops to a few minutes and even to few seconds when the viscosity becomes very small and when the d increases and becomes larger than a certain critical distance, typically of 6–7 nm. For $d = 7$ nm and $\eta = 10^2$ Pa·s, the chains take about 20 s to diffuse inside the space between to lamellae along the distance L . Such increase in d spacing can be ensured by simple thermal activated diffusion of the lamellae. The diffusion of intercalated clay lamellae (increase of the distance from approximately 4 to 7 nm) can occur by translation and by rotation. For a cylindrical geometry, the two modes of diffusion are characterized by the following two diffusion coefficients given respectively by⁹

$$D_T = \frac{k_B T \ln(L/t)}{2m\pi\eta L} \quad (8)$$

and

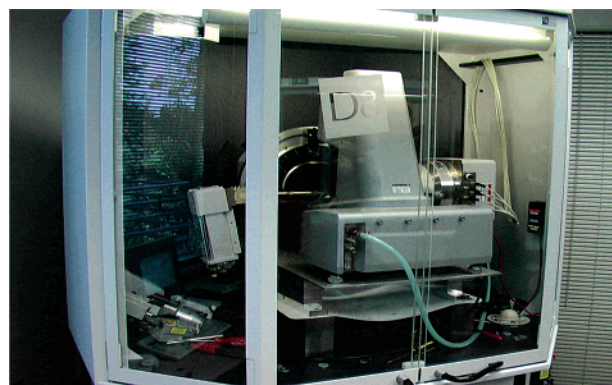
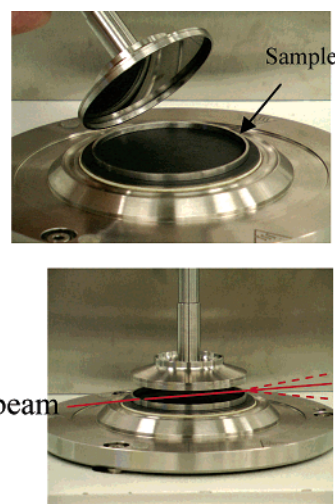
$$D_R = \frac{3k_B T b^2 \cos(\theta) [\ln(L/t) - 0.5]}{\pi\eta L^3} \quad (9)$$

The subscripts T and R stand for translation and rotation, respectively. The parameter m appearing in D_T takes the value 2 for a diffusion occurring parallel to the cylinder axis and 4 in the perpendicular direction. For flat plates, the expression of the diffusion coefficient is more complex than the above equations. For classical clay loading (2–5 wt %) the rotation can be ignored. For classical case of polymer melts, diffusion of lamellae from low d (let us say 4 nm) to higher values of d (let us say 7 nm) would require several hours for a matrix viscosity of 10^6 Pa·s, while it will require only few seconds for a matrix viscosity of 10^2 Pa·s.

Clearly, the mechanism of exfoliation is thought of here as a combination of diffusion of both polymeric chains and lamellae and mechanical delamination rather than the simplistic picture of peeling. There should be a balance between shear stresses that require high viscosity levels and diffusion process that necessitates rather low viscosity levels.

Experiments

To examine the mechanism of exfoliation, mixtures of 80 wt % of poly(ethylene-co-1-octene), 15 wt % of ethylene-octene maleic anhydride grafted with 0.2–0.5 wt % maleic anhydride, and 5 wt % of Cloisite 30B were prepared by mixing them in solid state. The obtained solid mixture was then compression molded at 150 °C for 1 min in a suited form that was used for shearing. The shear flow was applied using a state-of-the-art new experimental design. This consists of coupling an X-ray instrument from Bruker AXS Inc. directly with a Paar Physica rheometer. The X-ray device was

**Figure 2.** Coupling between wide-angle X-ray scattering (WAXS) and rheometry. Specifications of the coupling are explained in the text.**Figure 3.** Shearing device consists of two rings designed on the two plates. The upper rotating ring is conical, while the lower stationary one is flat. The sample in a ring form of 1 mm in width, 0.7 mm in thickness, and 24 mm in internal hollow radius is sheared when the upper plate rotates at a given rotation speed, the lower plate being stationary. During its trajectory, the X-ray beam touches the sample only at the exit on the right side.

connected to a new detector that allows acquisition of the output signal each 10 ms. The picture of Figure 2 illustrates the new instrument, where the rheometer was put inside the X-ray chamber. Here the rheometer is mounted on a moving support inclined at a given angle θ (typically 3°–5°). Such configuration ensures a peculiar trajectory for the X-ray beam. In fact, as shown in Figure 3, the sample in the form of a ring of 1 mm in width, 24 in diameter (inner diameter), and 0.7 mm in thickness is put between two metallic rings of 1 mm in width and 24 mm of inner diameter. The upper ring is conic with a cone angle of 0.1 rad, and the lower one is flat and maintained stationary. As in cone-and-plate geometry, the rotation of the upper conic ring with a given rotation speed induces homogeneous shear flow at constant shear rate within the ring sample. The X-ray beam enters from a hole at the left side of the lower plate and touches the sheared sample only at the right side. The experiments were conducted in the melt at 150 °C, where no degradation of the components was noticed.

Various flow histories were imposed on the polymer nanocomposite. Here we show only a typical experiment where the sample was first sheared at 0.02 s^{−1} for 15 min, and then the shear rate was increased at 0.6 s^{−1}. The variation of d_{001} was monitored on-line during shearing. X-ray diffractograms were acquired each second. The typical obtained results are shown in Figure 4.

As can be seen from the figure, the d_{001} increases in time and then reaches a steady-state value after 10 min of mild shearing (0.02 s^{−1}). Such an increase is mainly due to the diffusion step. Thereafter, shear rate was increased to a higher value (0.6 s^{−1}), which promoted

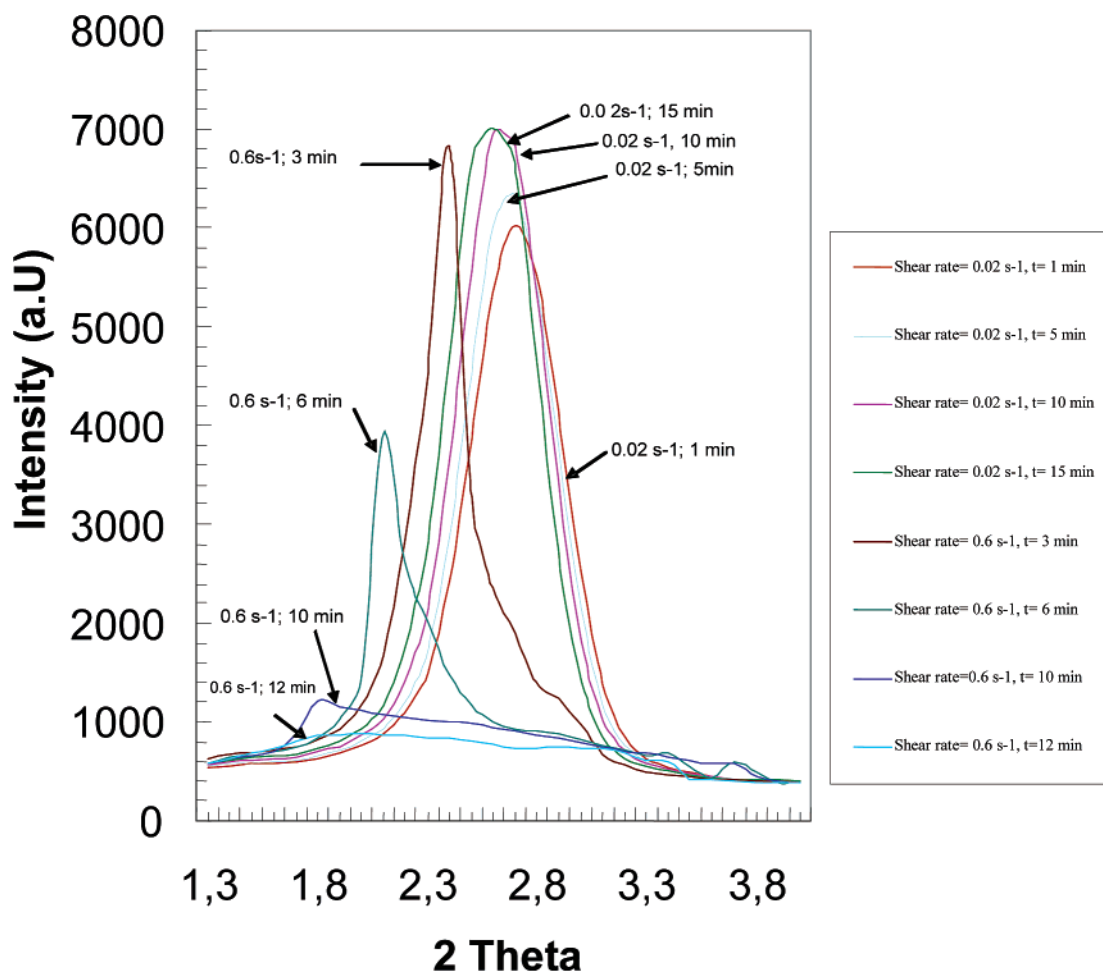


Figure 4. XRD pattern for modified of 80 wt % of poly(ethylene-*co*-1-octene), 15 wt % of ethylene-octene maleic anhydride grafted with 0.2–0.5 wt % maleic anhydride, and 5 wt % of Cloisite 30B during shear flow. Under quiescent conditions or under very mild shearing at 0.02 s^{-1} , the peak position of the plane (001) shifts to lower angles and then reaches a stable value. Upon increase of shear rate, the peaks shifts further to lower angles before disappearing completely after 15 min of shearing (exfoliation).

significantly the increase of d_{001} . A relatively high level of exfoliation is obtained after 12 min of shearing.

Clearly, based on both the above discussion and on the experimental results, a relatively high level of exfoliation is obtained when the sample was first subjected to static and isothermal conditions or at least under mild shearing conditions. This diffusion-controlled step results in a relative expansion of the clay lamellae. This expansion helps the polymeric chains to diffuse inside the confined space between the galleries. Thereafter, when shear intensity is increased, a higher degree of delamination of the various overlapped clay layers was obtained as revealed by the gradual shift in the 2θ peak to lower angles before it disappears completely. To the best of our knowledge, this is the first time that such kind of measurements is shown in the literature.

Effect of Degree of Exfoliation on Mechanical Properties

Exfoliated structure is presumed to be required to impart the nanocomposites with enhanced mechanical properties, and in many occasions intercalated or less exfoliated structures were discarded. To examine the effect of clay exfoliation level on the modulus of the nanocomposites, various samples were prepared with different levels of exfoliation. Such operation is based on the mechanism of exfoliation described in the previous section. This consists of mixing poly(ethylene-*co*-1-octene), 15 wt % of ethylene-octene maleic anhydride grafted with 0.2–0.5 wt % maleic anhydride, and 5 wt % of Cloisite 30B within a batch mixer at $150\text{ }^{\circ}\text{C}$. The different levels of exfoliation were obtained by varying the waiting time between the mild mixing

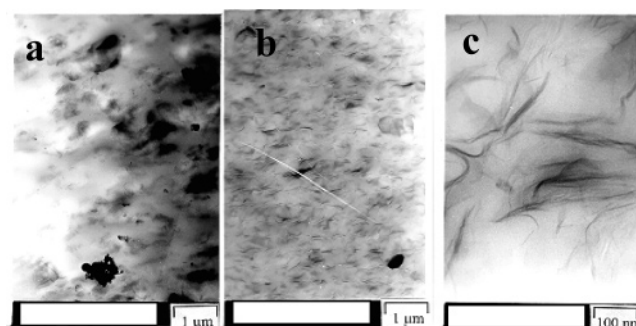


Figure 5. Three states of clay exfoliation within of poly(ethylene-*co*-1-octene)/ethylene-octene-*g*-maleic anhydride matrix are presented: (a) was obtained by rapid mixing of the components in a batch mixer under 60 rpm rotation speed in molten state, (b) was achieved by mixing the components in the same conditions but after 3 min of shearing at 10 rpm before increasing the rotation speed at 60 rpm, and (c) was obtained after 12 min of mild mixing at 10 rpm before increasing the rotation speed at 60 rpm.

(10 rpm) and the intensive shear conditions (60 rpm). The typical obtained structures are shown in Figure 5, and their corresponding modulus is reported in Figure 6.

The tensile modulus corresponding to the samples described in Figure 5 was measured with Instron testing machine in tensile mode. The experiments were conducted at 5 m/s of cross-head speed at room temperature. The presented results are average values obtained on 10 samples. The obtained average values

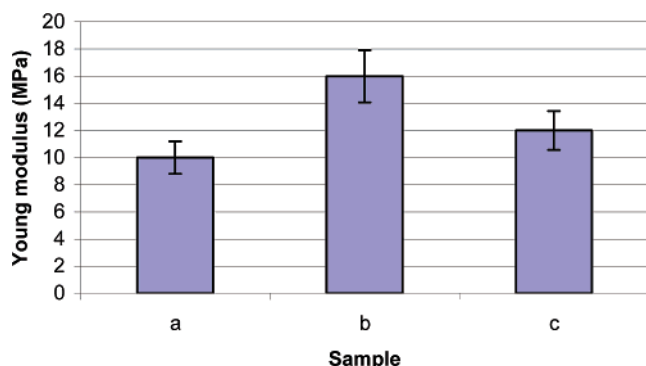


Figure 6. Young modulus (MPa) for the three samples shown in Figure 5.

are 10 MPa for sample a, 16 MPa for sample b, and 12 MPa for sample c. Normally, one expects sample c to exhibit the best mechanical properties in terms of tensile modulus. The results reveal in contrary that the best enhancement in modulus is exhibited by sample b that has intermediate level of exfoliation. The same results were obtained by Okamoto.¹⁴ Our interpretation is that clay particles are flexible and can bend under mechanical stresses, as can be seen in Figure 5. Mixing flexible lamellae with flexible polymeric chains does not change the overall flexibility of the mixture. To play their role as rigid fillers, it is then better to have some stacks of 10–20 clay layers dispersed within the polymeric matrix. Such stacks bend less than the individual flexible lamellae. Such a situation is equivalent to relatively rigid nanoparticles but with a thickness of 10–20 nm dispersed within the flexible thermoplastic polymer.

However, if one can maintain the clay lamellae well oriented in the direction by means of special processing (special die) of freezing such orientation in a cross-linked polymeric network such as in thermosets, then better mechanical properties can be expected. Another favorable case is that of a polymeric rigid matrix that has high specific interactions with the clay surface.

Concluding Remarks

The main findings of this work can be summarized by the followings:

It was found that the energy of interactions between clay lamellae is higher than the carbon–carbon bond energy when the interlamellar spacing is smaller than a critical distance. Shearing the nanocomposite at such high mechanical energy will degradate the polymeric matrix by breaking the C–C bonds rather than delaminate the clay lamellae.

The best level of exfoliation requires medium matrix viscosity. This is dictated by a balance between mechanical stresses that necessitate a high level of viscosity and a diffusion process that requires rather low medium viscosity. To reach high level of exfoliation, it is then recommended to mix the intercalated clay and the polymeric matrix in a molten state under mild shearing conditions. This allows expansion of the interspacing distance which facilitates polymer chains to diffuse into the confined space between the galleries. A high level of shearing applied after this period of diffusion leads to a high level of exfoliation.

It was also found that well-exfoliated structure in flexible matrixes such as the ones used in this work imparts the final nanocomposites with a tensile modulus that is smaller than that of medium exfoliated structure. Such a result was inferred to the flexibility of clay lamellae that bend under mechanical solicitations. Stacks of 10–20 lamellae bend less and reinforce better the flexible polymeric matrix.

Acknowledgment. This work was financially supported by the NSERC (Natural Sciences and Engineering Research Council of Canada) and Canada Research Chair on Polymer Physics and Nanomaterials and the Steacie Award grants.

References and Notes

- (1) Utracki, L. A. *Clay-Containing Polymeric Nanocomposites*; RAPRA Technology Ltd.: Shawbury, England, 2004; Vols. 1 and 2.
- (2) Dennis, H. R.; Hunter, D. L.; Chang, D.; Kim, S.; White, J. L.; Cho, J. W.; Paul, D. *Polymer* **2001**, *42*, 9513–9522.
- (3) Fornes, T. D.; Yoon, P. J.; Keskkula, H.; Paul, D. R. *Polymer* **2001**, *42*, 9929–9940.
- (4) Woo Kim S.; Ho Jo, W.; Sung Lee, M.; Bae Ko, M.; Young Jho, J. *Polym. J.* **2002**, *34*, 103–111.
- (5) Nassar, N.; Utracki, L. A.; Kamal, M. R. *Int. Polym. Proc.* **2005**, *4*, 423–431.
- (6) Tanoue, S.; Utracki, L. A.; Garcia-Rejon, A.; Tatibouet, J.; Cole, K. C.; Kamal, M. R. *Polym. Eng. Sci.* **2004**, *44*, 1046–1060.
- (7) Russel, W. B.; Saville, D. A.; Schowalter, W. R. *Colloidal Dispersions*; Cambridge University Press: New York, 1989.
- (8) de Gennes, P. G. *Scaling Concepts in Polymer Physics*; Cornell University Press: Ithaca, NY, 1999.
- (9) Doi, M.; Edwards, S. F. *The Theory of Polymer Dynamics*; Oxford University Press: New York, 1986.
- (10) Graessley, W. W. *J. Polym. Sci., Polym. Phys. Ed.* **1980**, *18*, 27–34.
- (11) Qiu, H.; Bousmina, M. *J. Rheol.* **2000**, *43*, 551–568.
- (12) Qiu, H.; Bousmina, M. *Macromolecules* **2000**, *33*, 6588–6594.
- (13) Chen, Y. L.; Graham, M. D.; de Paolo, J. J. *Phys. Rev. E* **2004**, *70*, 060901 (R).
- (14) Okamoto, M. *Rapra Rev. Rep.* **2003**, *14* (No. 7), Report 163.

MA052647F